
A PARAMETERIZED MODEL AND ANALYSIS
OF THE AERODYNAMIC FORCES
ENCOUNTERED BY UNGUIDED MODEL
ROCKETS DURING THEIR ASCENT PHASE

EXTENDED ESSAY

PHYSICS

INTERNATIONAL BACCALAUREATE



May 2021 Session

Contents

1	Introduction	3
1.1	Flight of a rocket	3
1.1.1	Ascent of a Rocket	4
1.2	Background Information	7
2	Methodology	9
2.1	Design of the Rockets	9
2.2	Flight Simulation and Data Collection	14
2.2.1	Results from Simulations	15
3	Creation of the Model	16
3.1	Calculation of Theoretical Values	16
3.1.1	At the Burnout instance	16
3.1.1.1	Burnout Velocity \vec{v}_b	16
3.1.1.2	Burnout Altitude \vec{h}_b	17
3.1.2	At the Apogee instance	18
3.1.2.1	Maximum Altitude	18
3.1.2.2	Coasting Time and Time to Apogee	18
3.2	Assignment of N	20
3.3	Calculation of the Reduction Factors	21
4	Analysis and Evaluation of the Model	23
4.1	Model Analysis	23
4.2	Percentage Deviations of Velocity and Height Magnitudes	25
4.2.1	Transonic and Supersonic Flight	28
4.3	Flight Stability	29
4.3.1	Aerodynamic Stability	29
4.3.2	Static Stability	30
4.4	Flight Trajectory Deviations	34
4.4.1	Two-Dimensional Flight	34
4.4.2	Implication of the Presence of Wind	36
5	Conclusion	37
6	Bibliography	38
7	Appendix	40
7.1	Derivation of Equation 3	40
7.2	Data and File Repository	41

Abstract

This paper focuses on the creation, analysis and evaluation of a parameterized model by giving each rocket a drag influence number to then calculate their performance in an environment where aerodynamical drag forces are taken into account. The model aims to simplify other methods of calculating such values for the performance of a rocket by eliminating the need for resorting to differential equations at the cost of some accuracy when comparing it to real-life applications. The model was created by obtaining factors from theoretical calculations neglecting aerodynamical forces, and computational simulations of rockets during their ascent phase. The outcome of this investigation yielded models with strong correlation coefficients demonstrating the relationship between a rockets design and the amount of drag it will experience.

1 Introduction

Numerical solutions for the two-dimensional flight of a rocket through a fluid such as air can be extremely complex to solve due to the implication of differential equations that may require computational methods to be resolved (Equation 3). This investigation will attempt to go around these differential equations by creating a simplified model achieved by making a base rocket, and changing its structural material density to obtain an array of rockets varying in mass with the same thrust and design, to then make a comparison of their theoretical and simulated values to obtain reduction factors (Equation 5) that can be easily applied to relatively simple equations that could then be applied to a wide array of rocket designs by parameterizing the rockets through a drag influence number N (Equation 6).

This investigation will attempt to create such model and then analyse its limitations as well as other external factors that could have not been considered during the design process or simulations, in the case where an experimental flight was done based on this model.

1.1 Flight of a rocket

The flight of a rocket is composed of two primary phases, the ascent and descent phase, where the rocket's motor burns a solid propellant due to chemical energy and expels it as a gas at a high velocity providing kinetic energy (E_K) to the rocket in the form of thrust accelerating the rocket forwards due to Newton's second and third laws of motion.

This investigation focuses solely on the ascent phase of a rocket, since its descent phase is irrelevant due to it not affecting performance, however, the following diagram portrays both.

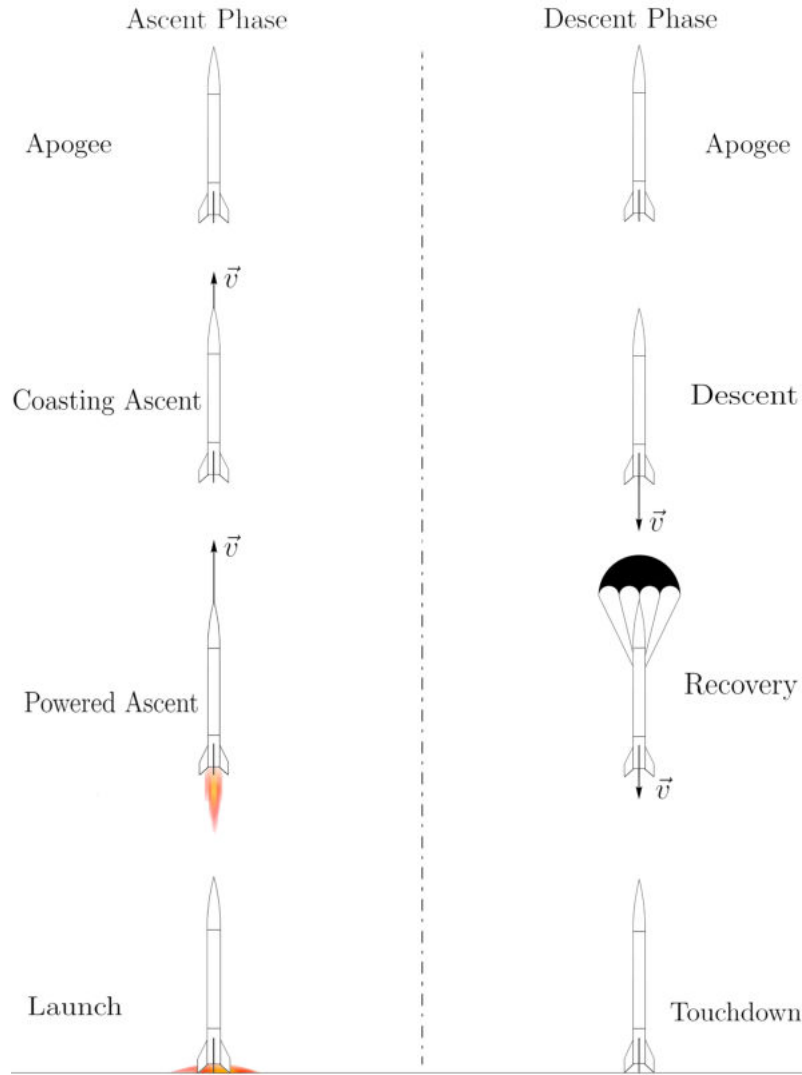


Figure 1: A diagram showing the ascent and descent phases of a rocket performing a vertical flight

1.1.1 Ascent of a Rocket

The flight of the rocket commences with its launch at t_0 , where the rocket's motor ignites.

As soon as the rocket lifts off from the ground, the powered ascent phase begins, which lasts for as long as the burn time of the motor t_b , at the instant where the motor depletes its fuel, the rocket reaches its burnout height \vec{h}_b and velocity \vec{v}_b . After the fuel has been burnt, the coasting flight of the rocket begins, where it continues to ascend due to inertia because of its 'stored' E_K , decelerating until the velocity reaches \vec{v}_0 after coasting for time t_c , reaching its apogee¹ \vec{h}_{max} , the distance between \vec{h}_b and \vec{h}_{max} for which the rocket coasts for is denoted as $\Delta\vec{h}_c$, and the time from

¹Maximum altitude

launch to reaching the apogee is denoted as t_{max} .

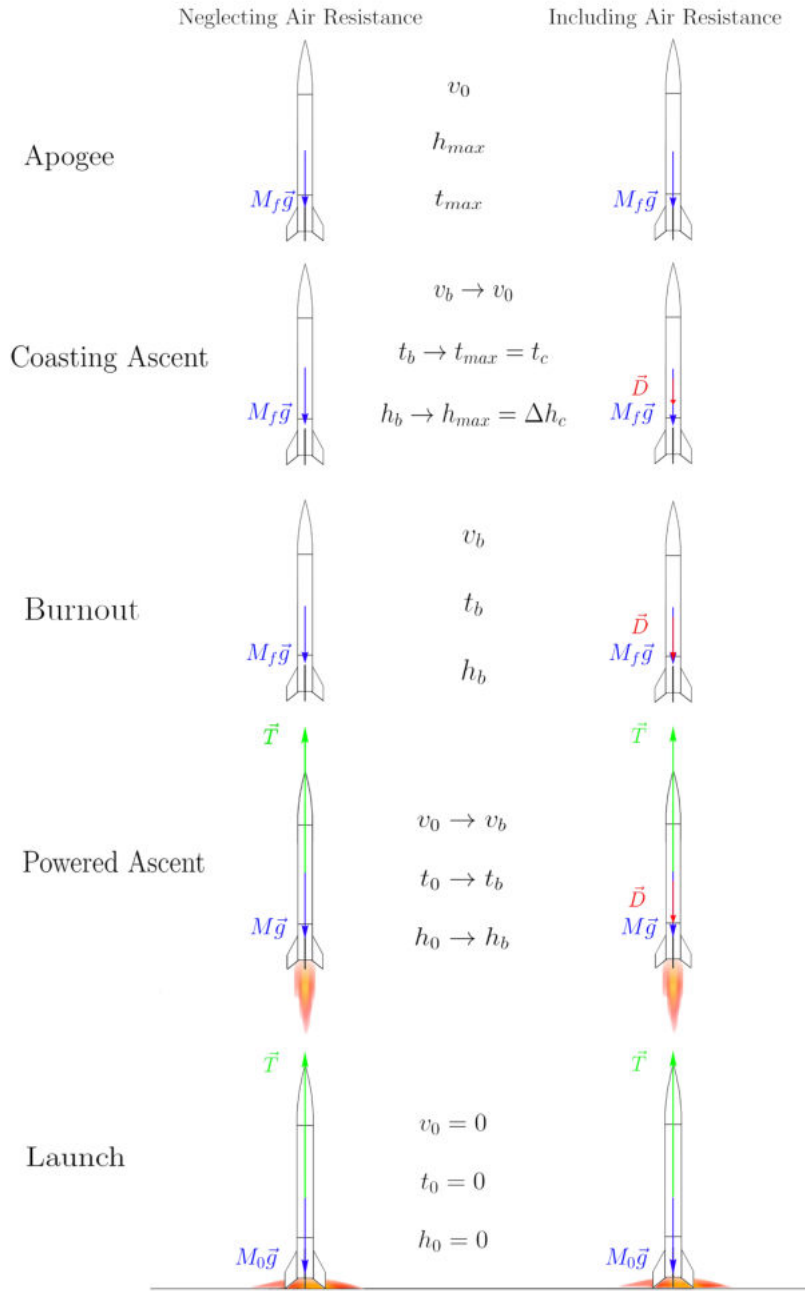


Figure 2: Diagram depicting free body diagrams for the rocket during its ascent, for both a an environment neglecting air resistance and including it

As we can see on figure 2, when air resistance is neglected, the only opposing force the rocket encounters is its weight ($\vec{W} = M\vec{g}$), however, when air resistance is taken into consideration, an additional opposing force is encountered, being the drag force (\vec{D}), this force significantly reduces the performance of rockets.

This loss in performance due to drag can be explained by comparing the equations of motion for both scenarios:

$$M \frac{d\vec{V}}{dt} = \vec{T} + \vec{W} + \vec{D} \quad (1)$$

Where \vec{T} is the rocket's instantaneous thrust and \vec{W} is the rockets instantaneous weight, both in N.

Since for an ideal flight, $\vec{D} = 0$, if we were to obtain a ratio between these, it would result in a drag loss $-\Delta\vec{D}$.

The equation for drag is given by the following equation:

$$\vec{D} = C_D \frac{1}{2} \rho \vec{V}^2 A \quad (2)$$

Where C_D is the rockets drag coefficient, ρ is the air density in kgm^{-3} at the rocket's instantaneous height, \vec{V} is rocket's instantaneous velocity in ms^{-1} , and A is the frontal area of the rocket in m^2 .

As we can see from this equation, as velocity doubles, the drag force is quadrupled. Since rockets achieve very high velocities, this force becomes very significant. For this reason, there cannot be a generalized reduction of performance for all rocket's, since it is heavily dependent on the rocket's specifications.

Calculating the velocity differential of the rocket involves the following differential equation²

$$d\vec{V} = -\vec{w} \frac{dM}{M} - \vec{g} dt - \frac{\vec{D}}{M} dt \quad (3)$$

²The derivation of Equation 3 is shown in the appendix.

Where \vec{w} is the exhaust velocity of the expelled gas from the motor in ms^{-1} , M is the rockets instantaneous mass in kg and \vec{g} is the gravitational acceleration in ms^{-2} .

1.2 Background Information

The performance of a rocket is given by the maximum velocity and altitude it achieves. The maximum theoretical performance a rocket is obtained when there is no drag opposing the rockets motion. If we approximate the gravitational field to be homogeneous since the change can be neglected, calculating these theoretical values becomes a straight-forward task involving simple equations.

The ideal and simplest method to approximate the rockets performance when affected by drag would be by applying a reduction factor to the theoretical values where:

$$\text{Value adjusted for Drag} = \text{Theoretical Value} \times \text{Reduction Factor} \quad (4)$$

To obtain these reduction factors, since launching several rockets and accurately recording their height and velocity wasn't an option, the rocket simulator OpenRocket (Niskanen) was utilized, which allowed us to run simulations with the same specifications as the rockets used in the theoretical calculations, with drag being taken into account. This would allow for performance reduction factors to be obtained and then applied for a drag adjusted model through the following equation:

$$\text{Reduction Factor} = \frac{\text{Simulated Value}}{\text{Theoretical Value}} \quad (5)$$

The relevant reduction factors were dictated by those values that were affected by drag, being:

- At the Burnout instance
 - Burnout Velocity Factor: f_{v_b}
 - Burnout Altitude Factor: f_{h_b}

- At the Apogee instance
 - Altitude Gain from Coasting Factor: $f_{\Delta h_c}$
 - Maximum Altitude Factor: $f_{h_{max}}$
 - Coasting Time Factor: f_{t_c}
 - Time to Apogee Factor: $f_{t_{max}}$

Figure 3: Factors of the variables that will be calculated in order to create the model.

These factors would then be plotted against a parameter calculated for each rocket which is the rocket's Drag Influence Number N (Nakka), where this parameter would be the x axis of the graph, and the factors would be the y axis. A line of best fit would be then obtained for each factor to obtain our model.

Parameter N is obtained through the following equation:

$$N = \frac{C_D \varnothing^2 \vec{v}_b^2 \times 10}{M_f} \quad (6)$$

Where \varnothing is the diameter of the rocket in m.

Assigning this parameter N would allow for different rockets with different specifications to use it, rather than having it only work with one design.

2 Methodology

2.1 Design of the Rockets

The rockets were designed within the simulator.

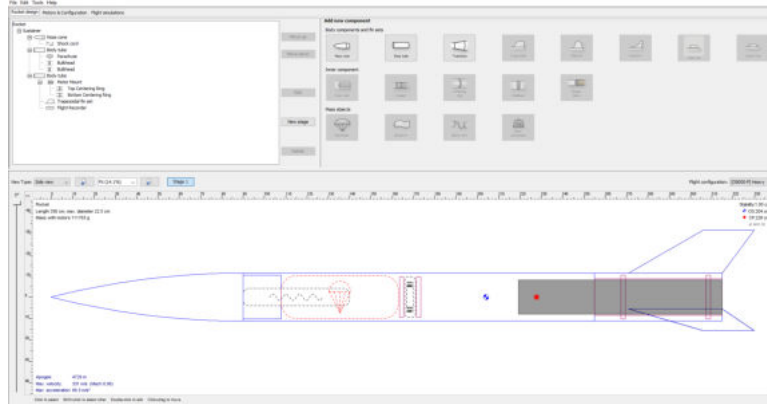


Figure 4: A screen capture from the simulator *OpenRocket* showing the rocket assembly configuration menu

In order to change the drag force acting on each rocket, the density of the rocket's structural material was changed, every other design aspect remained unchanged for all variations, including its motor, shape, payload, etc.

By keeping these constant, the rockets would have the same \vec{T} and C_D , but achieve different maximum velocities and apogees, allowing for a decent range of parameter N assigned to each rocket.

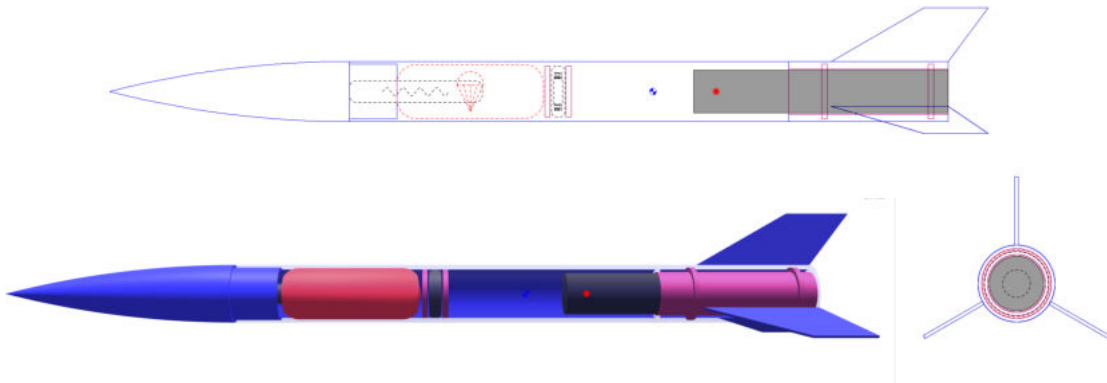


Figure 5: Diagrams of rocket including non-structural components from the design menu

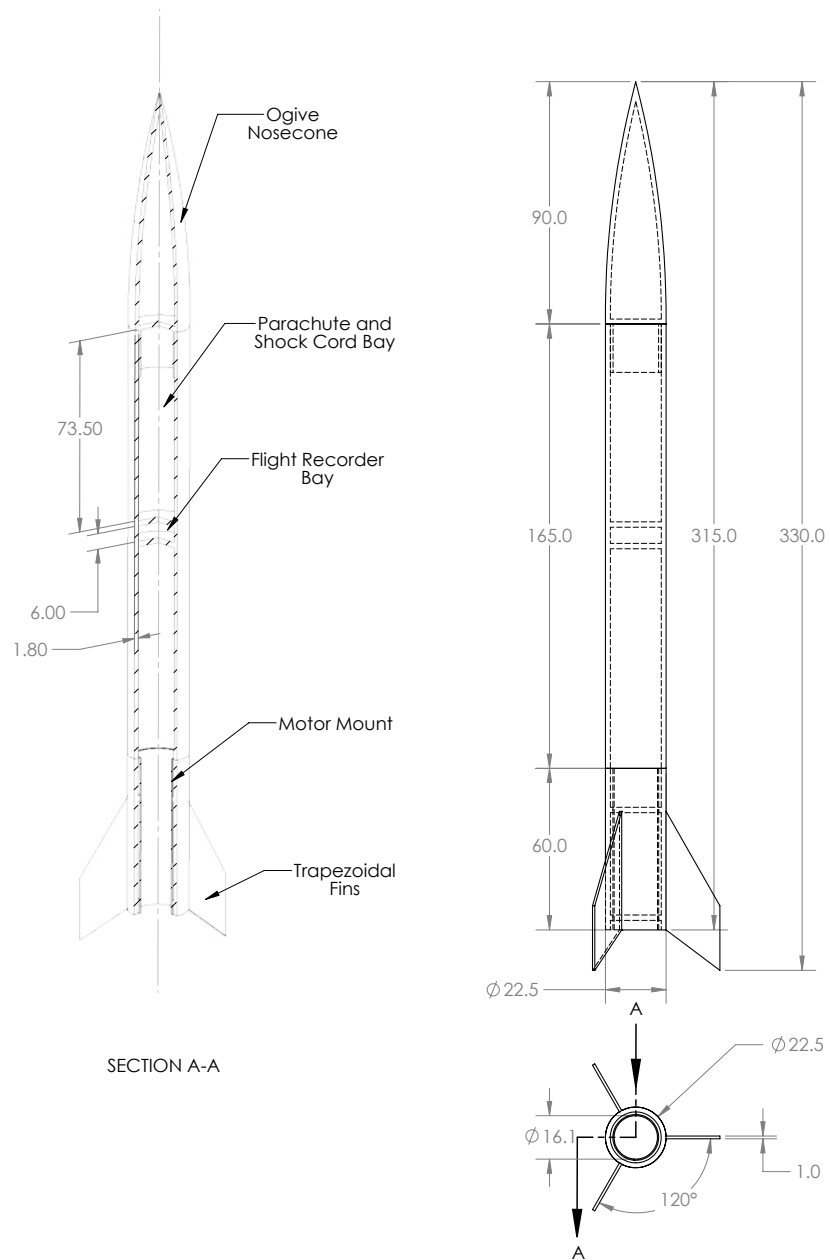


Figure 6: Diagram showing dimensions (in cm) and labels of the rocket's structure

The following parameters were shared by all rockets:

Common Parameters		
Parameter		Value
Diameter	\emptyset	0.225 m
Drag Coefficient	C_D	0.36
Total Impulse	I	40690 Ns ⁻¹
Average Thrust	T	8034.5 N
Specific Impulse	I_{sp}	225.6 s
Propellant Mass	M_p	18.61 kg
Mass Flow Rate	\dot{m}	3.635 kgs ⁻¹
Exhaust Velocity	w	2210.5 ms ⁻¹
Burn Time	t_b	5.12 s

Table 1: Parameters shared in common by all rockets.

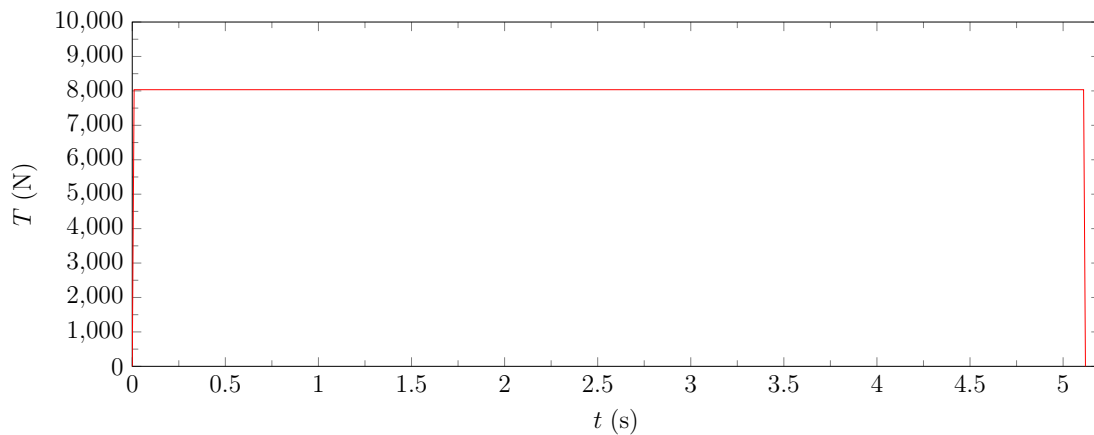


Figure 7: Graph showing the thrust provided by the motor against time

The mass flow rate was calculated using the equation:

$$\dot{m} = \frac{dM_p}{dt_b} \quad (7)$$

For this motor;

$$\dot{m} = \frac{18.61}{5.12} = 3.635 \text{ kg} \cdot \text{s}^{-1}$$

The exhaust velocity was calculated using the equation:

$$\vec{w} = \frac{\vec{T}}{\dot{m}} \quad (8)$$

For this motor;

$$\vec{w} = \frac{8034.5}{3.635} = 2210.5 \text{ ms}^{-1}$$

A total of 18 different variations of the rocket were made, labelled A-R, each with a different structural material density.

Rocket Specific Parameters						
Rocket	Structural Density	Initial Mass	Final Mass	Initial Weight	Thrust to Weight	Mass Ratio
	ρ_s (gcm ⁻³)	M_0 (kg)	M_f (kg)	W_0 (N)	Ψ_0	Λ
A	0.76	69.15	50.54	677.6	11.86	1.368
B	0.85	72.85	54.24	714.0	11.25	1.343
C	0.95	76.75	58.14	752.1	10.68	1.320
D	1.00	78.69	60.08	771.2	10.42	1.310
E	1.05	80.63	62.02	790.1	10.17	1.300
F	1.10	82.58	63.97	809.3	9.93	1.291
G	1.19	86.07	67.46	843.5	9.53	1.276
H	1.20	86.46	67.85	847.3	9.48	1.274
I	1.30	90.36	71.75	885.6	9.07	1.259
J	1.39	93.85	75.24	919.8	8.74	1.247
K	1.50	98.13	79.52	961.7	8.35	1.234
L	1.60	102.04	83.43	1000.0	8.03	1.223
M	1.70	105.93	87.32	1038.1	7.74	1.213
N	1.78	109.03	90.419	1068.5	7.52	1.206
O	1.90	113.71	95.10	1114.3	7.21	1.196
P	2.00	117.60	98.99	1152.5	6.97	1.188
Q	2.70	144.83	126.22	1419.3	5.66	1.147
R	4.50	214.86	196.25	2105.6	3.82	1.095

Table 2: Parameters specific to each rocket iteration.

The initial mass, was given by the simulator when designed. It can be calculated through the following equation:

$$M_0 = M_s + M_c + M_p \quad (9)$$

Where M_s is the mass of the structure, given by:

$$M_s = \rho_s V \quad (10)$$

V being the rockets volume. ρ_s the structural material payload, and M_c is the mass of the payloads carrying, being any other non-structural components.

The final mass was calculated with the equation:

$$M_f = M_0 - M_p \quad (11)$$

The mass ratio (Λ), which states how much heavier the rocket is with propellant than without, was calculated with the equation:

$$\Lambda = \frac{M_0}{M_f} \quad (12)$$

The thrust to weight ratio (Ψ_0), indicating the rockets how much thrust the rocket provides in relation to its initial weight, as a measure of its initial performance was calculated with the equation:

$$\Psi_0 = \frac{\vec{T}}{\vec{W}_0} = \frac{\vec{T}}{M_0 \vec{g}} \quad (13)$$

2.2 Flight Simulation and Data Collection

In order to collect the performance values that we would then compare with our theoretical values, we ran simulations for each rocket in Table 2 under the exact same conditions, the monitored variables are shown in the following table:

Controlled Variables	Independent Variables	Dependent Variables
The same launch location was used for each iteration, in order to maintain the initial gravitational acceleration as constant as possible.	The Structural Density (ρ_{mat}) of the structural material was for each iteration of the rockets was varied. (Table 2)	The initial and final mass of each iteration of the rocket. (Table 2)
The same atmospheric conditions were present for all iterations).		Burnout Velocity (\vec{v}_b) Burnout Altitude (\vec{h}_b)
The windspeed for each flight was null (0ms^{-1}).		Coasting Altitude Gain ($\Delta\vec{h}_c$) Maximum Altitude (Apogee) (\vec{h}_{max})
The structural design for each iteration remained constant, as well as their internal components and the mass of those: parachute, shock cord, and flight recorder. (Figure 6)		Coasting Time (t_c) Time to Apogee (t_{max})
The same motor was used for each iteration, providing the same amount of thrust (T) for each. (Table 1)		(Table 4 (Simulation Data), Table 5(Theoretical Data))
The launch orientation was the same for each iteration, each rocket being launched perpendicular to the ground at a 0° angle with the vertical.		

Table 3: Table showing the controlled, independent, and dependent variables which were worked with for and during the investigation.

Switching between rockets for the simulations was a simple process since all that had to be done was modify the structural density of each component to match the desired one in the simulator.

2.2.1 Results from Simulations

The following table includes the values for the simulated flights of each rocket necessary to then calculate the factors, after having been filtered from all unprocessed data extracted from the simulation.

Simulation Data						
Rocket	Burnout Velocity \vec{v}_b (ms^{-1})	Burnout Altitude \vec{h}_b (m)	Coasting Alt. Increase $\Delta\vec{h}_c$ (m)	Apogee Alt. \vec{h}_{max} (m)	Coast Time t_c (s)	Total Time t_{max} (s)
A	551.9	1437.6	5983.8	7421.4	31.05	36.18
B	522.6	1363.8	5769.2	7133	30.80	35.94
C	494.7	1293.5	5541.9	6835.4	30.45	35.59
D	481.8	1260.8	5428.6	6689.4	30.30	35.45
E	469.4	1229.6	5316.0	6545.6	30.10	35.25
F	457.5	1200.9	5203.2	6404.1	29.90	35.06
G	437.6	1150.4	5005.2	6155.6	29.50	34.66
H	435.5	1145.1	4983.4	6128.5	29.45	34.61
I	415.3	1093.8	4773.8	5867.6	29.05	34.22
J	400.2	1032.2	4623.1	5655.3	28.75	33.88
K	381.7	984.7	4436.6	5421.3	28.30	33.43
L	366.2	944.8	4278.4	5223.2	27.95	33.09
M	351.8	908.4	4121.6	5030	27.55	32.69
N	340.9	880.3	3993.1	4873.4	27.20	32.35
O	325.4	840.8	3791.2	4632	26.65	31.80
P	313.2	811.0	3624.8	4435.8	26.15	31.31
Q	245.8	627.0	2591.4	3218.4	22.50	27.64
R	147.7	378.1	1064.7	1442.8	14.70	19.85

Table 4: Simulation data retrieved for each rocket.

3 Creation of the Model

In order to model the loss in performance due to drag for the rockets, a comparison between their simulated flight and an ideal theoretical flight had to be done.

3.1 Calculation of Theoretical Values

The theoretical values calculated would be those where the rocket is flying in an ideal environment, where air resistance is neglected, and gravity was taken as constant $\vec{g} = 9.80 \text{ ms}^{-2}$

3.1.1 At the Burnout instance

3.1.1.1 Burnout Velocity \vec{v}_b

The theoretical burnout velocity was calculated with the following equation:

$$\vec{v}_b = \vec{w} \cdot \ln \Lambda - \vec{g} \cdot t_b \quad (14)$$

Derivation of Equation 14 (David)

To find the rocket's ideal burnout velocity, $d\vec{V}$ (Equation 3, without drag) is integrated from v_0 to v_b :

$$\int_{v_0}^{v_b} d\vec{V} = -\vec{w} \frac{dM}{M}$$

Therefore

$$\begin{aligned} \vec{v}_b &= \vec{w} \ln \frac{M_0}{M_f} \\ &= \vec{w} \ln \Lambda \end{aligned}$$

If we now add the external forces drag and gravity:

$$\vec{v}_b = \vec{w} \ln \Lambda - \int_{t_0}^{t_b} \vec{g} dt - \int_{t_0}^{t_b} \frac{\vec{D}}{M} dt$$

If drag is neglected, it then becomes:

$$\vec{v}_b = \vec{w} \ln \Lambda - \int_{t_0}^{t_b} \vec{g} dt$$

Integration then yields:

$$\vec{v}_b = \vec{w} \ln \Lambda - \vec{g}t_b$$

3.1.1.2 Burnout Altitude \vec{h}_b

The theoretical burnout altitude was calculated with the following equation:

$$\vec{h}_b = \vec{w} \cdot t_b \left(1 - \frac{\ln \Lambda}{\Lambda - 1}\right) - \vec{g} \cdot \frac{t_b^2}{2} \quad (15)$$

Derivation of Equation 15 (Ambrosius, Hamann, and Wakker)

To find the rocket's burnout altitude, we integrate its velocity from t_0 to t_b under ideal conditions with no gravitational losses.

$$\vec{h}_b = \int_{t_0}^{t_b} \vec{V} dt = - \int_{t_0}^{t_b} \vec{w} \ln \frac{M_f}{M_0} dt$$

Since \dot{m} ($-\frac{dM}{dt}$) and \vec{w} are constant:

$$\vec{h}_b = \frac{\vec{w}}{\dot{m}} \int_{M_0}^{M_f} \ln \frac{M_f}{M_0} dM = \frac{\vec{w}}{\dot{m}} \int_{M_0}^{M_f} \left(\ln M_f - \ln M_0 \right) dM$$

Integration then yields:

$$\vec{h}_b = \frac{\vec{w}(M_0 - M_f)}{\dot{m}} \left(1 + \frac{M_f}{M_0 - M_f} \ln \frac{M_f}{M_0}\right)$$

Which is the same as:

$$\vec{h}_b = \vec{w}t_b \left(1 - \frac{\ln \Lambda}{\Lambda - 1}\right)$$

To get the burnout altitude of a rocket with gravitational losses:

$$\vec{h}_b = \vec{w}t_b \left(1 - \frac{\ln \Lambda}{\Lambda - 1}\right) - \int_{t_0}^{t_b} \vec{g}t dt$$

Which yields:

$$\vec{h}_b = \vec{w} \cdot t_b \left(1 - \frac{\ln \Lambda}{\Lambda - 1} \right) - \vec{g} \cdot \frac{t_b^2}{2}$$

3.1.2 At the Apogee instance

3.1.2.1 Maximum Altitude

The theoretical maximum altitude was calculated with the following equation:

$$\vec{h}_{max} = \vec{h}_b + \Delta \vec{h}_c \quad (16a)$$

Where

$$\Delta \vec{h}_c = \frac{\vec{v}_b^2}{2\vec{g}} \quad (16b)$$

3.1.2.2 Coasting Time and Time to Apogee

The theoretical total time was calculated with the following equation:

$$t_{max} = t_b + t_c \quad (17a)$$

Where

$$t_c = \frac{\vec{v}_b}{\vec{g}} \quad (17b)$$

The following table shows the theoretical calculated values for each rocket.

Theoretical Data						
Rocket	Burnout Velocity	Burnout Altitude	Coasting Alt. Increase	Apogee Alt.	Coast Time	Total Time
	\vec{v}_b (ms^{-1})	\vec{h}_b (m)	$\Delta\vec{h}_c$ (m)	\vec{h}_{max} (m)	t_c (s)	t_{max} (s)
A	642.9	1553.2	21085.6	22638.8	65.6	70.7
B	601.8	1458.8	18479.7	19938.4	61.4	66.5
C	563.7	1370.5	16212.9	17583.4	57.5	62.6
D	546.3	1329.9	15226.3	16556.2	55.7	60.9
E	529.9	1291.7	14327.3	15619.0	54.1	59.2
F	514.3	1255.1	13493.2	14748.3	52.5	57.6
G	488.3	1194.2	12166.9	13361.1	49.8	55.0
H	485.6	1187.8	12030.7	13218.4	49.6	54.7
I	459.6	1126.4	10775.6	11902.0	46.9	52.0
J	438.3	1076.1	9803.4	10879.5	44.7	49.8
K	414.6	1019.8	8771.3	9791.0	42.3	47.4
L	394.9	972.8	7957.8	8930.6	40.3	45.4
M	376.9	929.7	7247.5	8177.1	38.5	43.6
N	363.5	897.6	6742.6	7640.3	37.1	42.2
O	344.9	852.8	6068.8	6921.6	35.2	40.3
P	330.6	818.4	5577.1	6395.6	33.7	38.9
Q	253.8	632.0	3287.7	3919.7	25.9	31.0
R	150.1	376.5	1149.2	1525.7	15.3	20.4

Table 5: Theoretical calculated data retrieved for each rocket.

3.2 Assignment of N

Since the theoretical velocity of the rockets is now known, the Drag Influence Number (N) was then calculated and assigned to each variation of the rocket using Equation 6.

Rocket	Final Mass M_f (kg)	Theoretical Burnout Velocity \vec{v}_b (ms ⁻¹)	Drag Influence Number N (m ⁴ s ⁻² kg ⁻¹)
A	50.54	642.9	1490.4
B	54.24	601.8	1216.9
C	58.14	563.7	996.2
D	60.08	546.3	905.3
E	62.02	529.9	825.3
F	63.97	514.3	753.5
G	67.46	488.3	644.2
H	67.85	485.6	633.4
I	71.75	459.6	536.4
J	75.24	438.3	465.4
K	79.52	414.6	394.0
L	83.43	394.9	340.7
M	87.32	376.9	296.5
N	90.42	363.5	266.4
O	95.10	344.9	228.0
P	98.99	330.6	201.3
Q	126.22	253.8	93.0
R	196.25	150.1	20.9

Table 6: Table showing the variables needed for the calculation of its Drag Influence Number and its value.

3.3 Calculation of the Reduction Factors

Using Equation 5 for each pair of corresponding simulated and theoretical values, the following calculated reduction factors are shown in the following table:

Calculated Factors						
Drag Influence Number	Burnout Velocity Factor	Burnout Altitude Factor	Coasting Alt. Increase Factor	Apogee Alt. Factor	Coast Time Factor	Total Time Factor
N	f_{v_b}	f_{h_b}	$f_{\Delta h_c}$	$f_{h_{max}}$	f_{t_c}	$f_{t_{max}}$
1490.4	0.86	0.93	0.28	0.33	0.47	0.51
1216.9	0.87	0.93	0.31	0.36	0.50	0.54
996.2	0.88	0.94	0.34	0.39	0.53	0.57
905.3	0.88	0.95	0.36	0.40	0.54	0.58
825.3	0.89	0.95	0.37	0.42	0.56	0.60
753.5	0.89	0.96	0.39	0.43	0.57	0.61
644.2	0.90	0.96	0.41	0.46	0.59	0.63
633.4	0.90	0.96	0.41	0.46	0.59	0.63
536.4	0.90	0.97	0.44	0.49	0.62	0.66
465.4	0.91	0.96	0.47	0.52	0.64	0.68
394.0	0.92	0.97	0.51	0.55	0.67	0.70
340.7	0.93	0.97	0.54	0.58	0.69	0.73
296.5	0.93	0.98	0.57	0.62	0.72	0.75
266.4	0.94	0.98	0.59	0.64	0.73	0.77
228.0	0.94	0.99	0.62	0.67	0.76	0.79
201.3	0.95	0.99	0.65	0.69	0.78	0.81
93.0	0.97	0.99	0.79	0.82	0.87	0.89
20.9	0.98	1.00	0.93	0.95	0.96	0.97

Table 7: Factors calculated for each rocket assigned to their corresponding Drag Influence Number

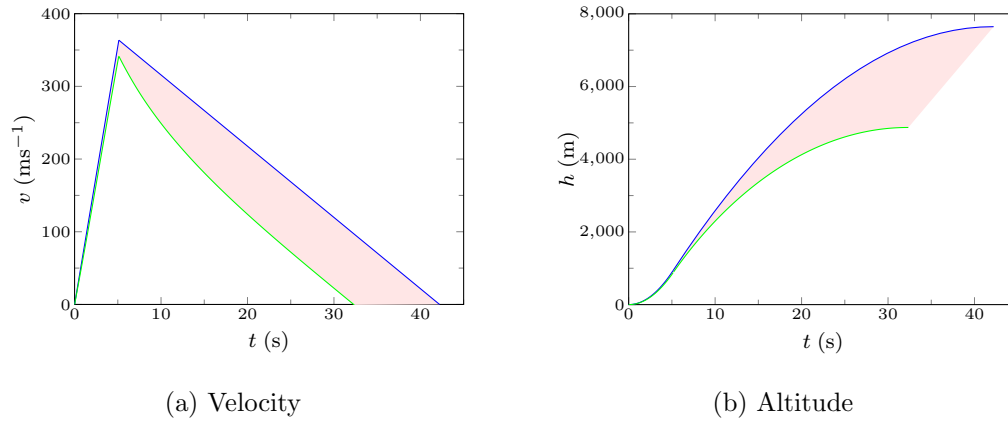


Figure 8: Graphs comparing velocity time and height time functions for **theoretical** and **simulated** flight of rocket N with Drag Influence Number of 266.4

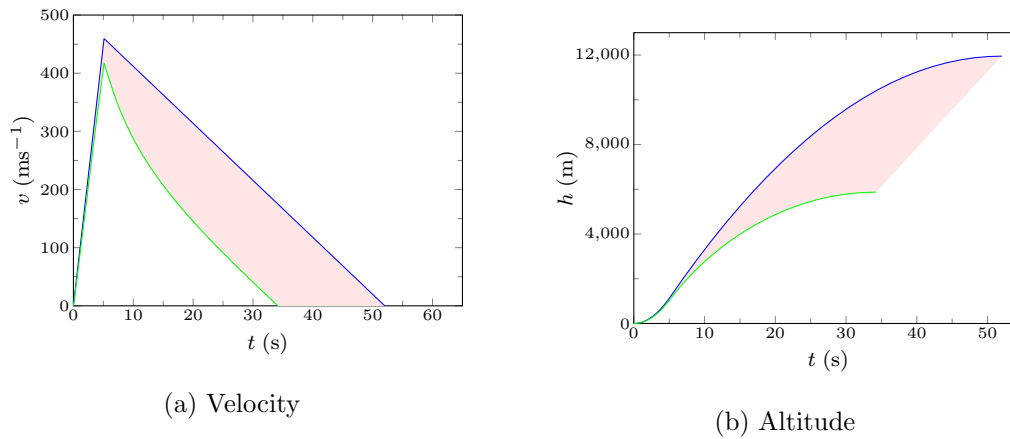


Figure 9: Graphs comparing velocity time and height time functions for **theoretical** and **simulated** flight of rocket I with Drag Influence Number of 536.4

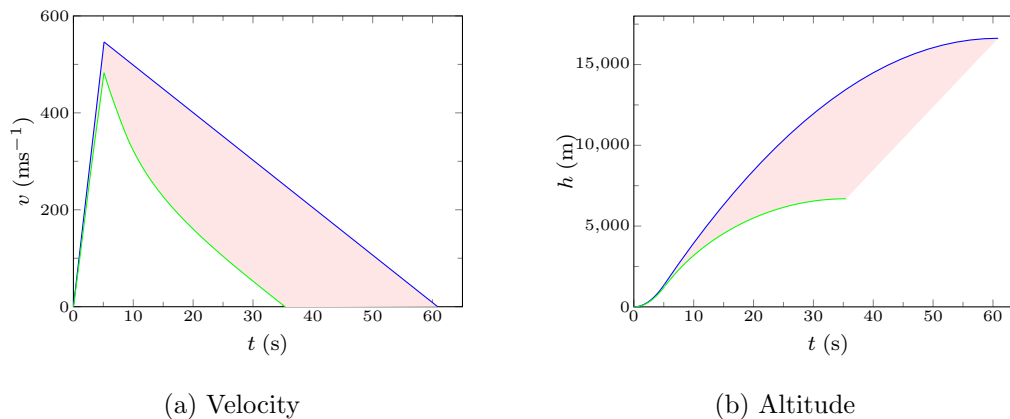
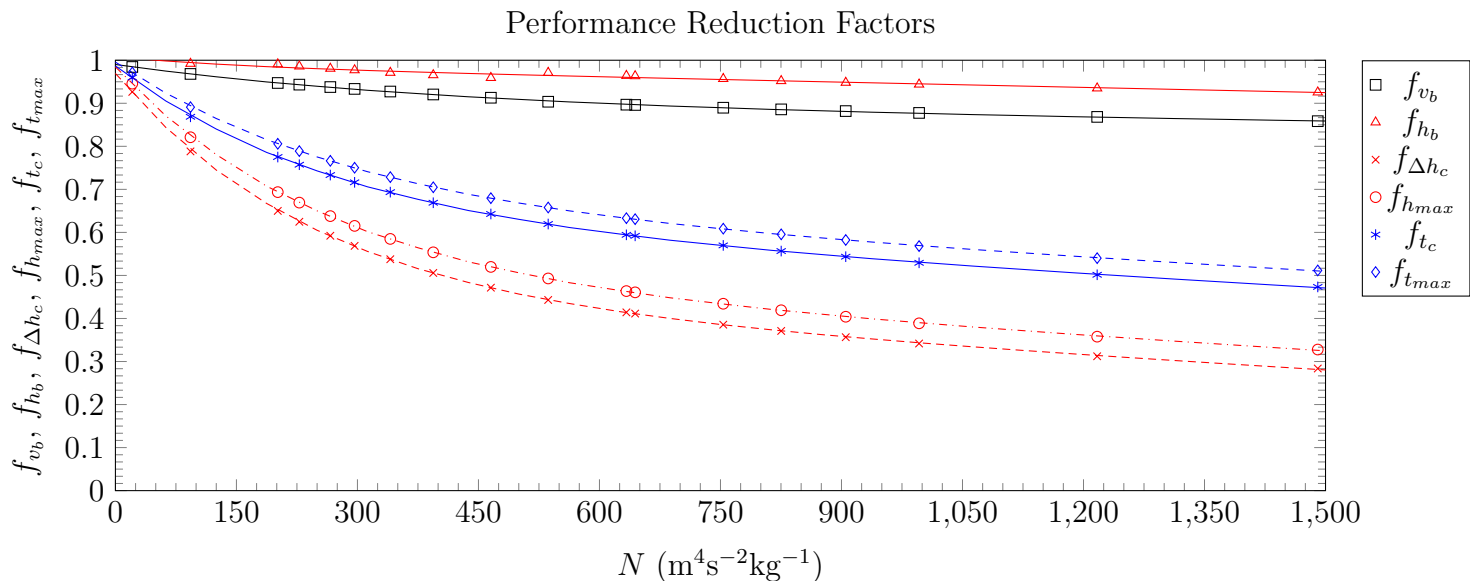


Figure 10: Graphs comparing velocity time and height time functions for the **theoretical** and **simulated** flight of rocket D with Drag Influence Number of 905.3

4 Analysis and Evaluation of the Model

4.1 Model Analysis

A function for the line of best fit was assigned for each corresponding factor, the results are as shown below:



$$\text{— } f_{vb}(N) = 0.8899 + 0.1992 \times 0.9976^N - 2.261 \times 10^{-5}N \quad (18)$$

$$\text{— } f_{hb}(N) = 0.9853 + 0.02238 \times 0.9942^N - 4.032 \times 10^{-5}N \quad (19)$$

$$\text{--- } f_{\Delta hc}(N) = 0.4445 + 0.5248 \times 0.9959^N - 1.01 \times 10^{-4}N \quad (20)$$

$$\text{-.-. } f_{h_{max}}(N) = 0.4923 + 0.4923 \times 0.9961^N - 1.126 \times 10^{-4}N \quad (21)$$

$$\text{— } f_{tc}(N) = 0.6607 + 0.3349 \times 0.9965^N - 1.021 \times 10^{-4}N \quad (22)$$

$$\text{--- } f_{t_{max}}(N) = 0.6254 + 0.3613 \times 0.9963^N - 1.04 \times 10^{-4}N \quad (23)$$

Figure 11: Scatter plot of reduction factors (Table 7) with their lines of best fit and the equations for the lines of best fit of each respective factor.

When analysing the model, we notice that they all have the same function model, being the *Exponential Plus Linear* function, given by the following equation:

$$f(N) = a + br^N + cN \quad (24)$$

This means that the performance of a rocket will decrease exponentially as its drag influence number decreases, until arriving at a boundary where it linearises.

The red shaded areas in figures 8(a,b), 9(a,b) and 10(a,b) represent the performance loss due to drag ($-\Delta\vec{D}$). An observation made, where as N increases, $-\Delta\vec{D}$ became significantly larger.

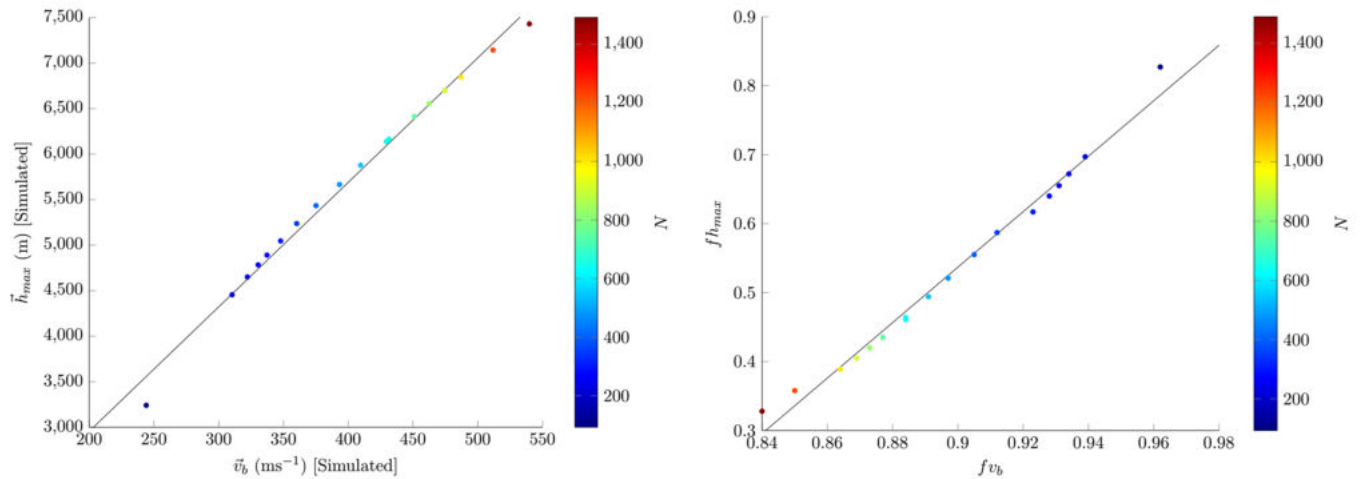


Figure 12: Burnout velocity vs. Maximum height plot (left) with Drag Influence colourbar and Burnout velocity factor vs. Maximum height factor plot with Drag Influence Number colourbar (right).

These graphs clearly show the significant performance loss suffered by rockets with a high N value.

For our trials, the main feature that increased this parameter was the overall mass of the rocket, where rockets with lower structural densities performed the best, as it can be observed by expanding Equation 6:

$$N = \frac{C_D \varnothing^2 \left(\frac{\bar{T}}{\bar{m}} \ln \frac{M_0}{M_f} - \bar{g} t_b \right)^2 \times 10}{\left[\left(\rho_s V + M_c + M_p \right) - M_p \right]} \quad (25)$$

Even though rockets with high N numbers achieved the greatest velocities and altitudes, these suffered tremendous losses in performance when compared to their respective theoretical values, this is primarily due to: $\vec{D} \propto \vec{V}^2$ (Equation 2). This shows how it was not the mass that directly affected the drag force, but rather, the higher velocities lightweight rockets could achieve.

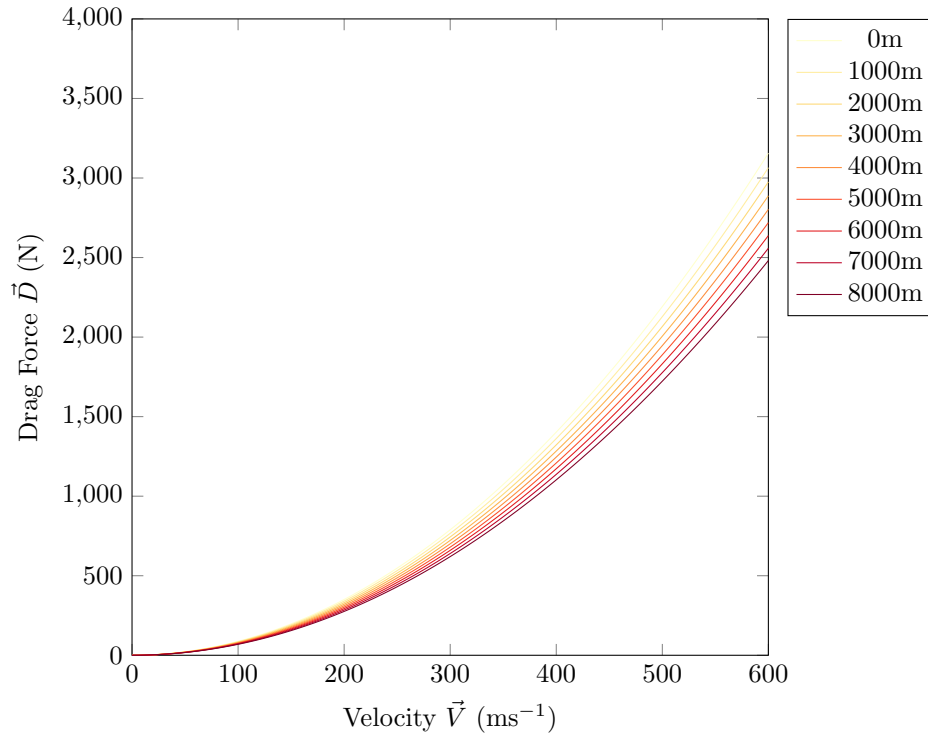


Figure 13: Drag force (Equation 2) acting upon the rocket with reference area $A = 0.039761\text{m}^2$ at different altitudes defined by the air density at these altitudes defined by the ISA (Young) against its instantaneous velocity of the rocket.

4.2 Percentage Deviations of Velocity and Height Magnitudes

The percentage deviation was calculated to obtain the difference between the simulations and theoretical calculations through the following equation:

$$\text{Percentage Deviation}(\sigma) = \frac{\text{Theoretical Value} - \text{Simulated Value}}{\text{Simulated Value}} \times 100 \quad (26)$$

Percentage Deviation		
N	$\sigma \vec{v}_b$	$\sigma \vec{h}_b$
1490	16.5%	205.0%
1220	15.2%	179.5%
996	13.9%	157.2%
905	13.4%	147.5%
825	12.9%	138.6%
753	12.4%	130.3%
644	11.6%	117.1%
633	11.5%	115.7%
536	10.7%	102.8%
465	9.5%	92.4%
394	8.6%	80.6%
341	7.8%	71.0%
296	7.1%	62.6%
266	6.6%	56.8%
248	6.0%	49.4%
228	5.6%	44.2%
201	3.3%	21.8%
93	1.6%	5.7%

Table 8: Graphs showing scatter plots alongside their lines of best fit for burnout velocity $\sigma \vec{v}_b$ and $\sigma \vec{h}_{max}$ against N .

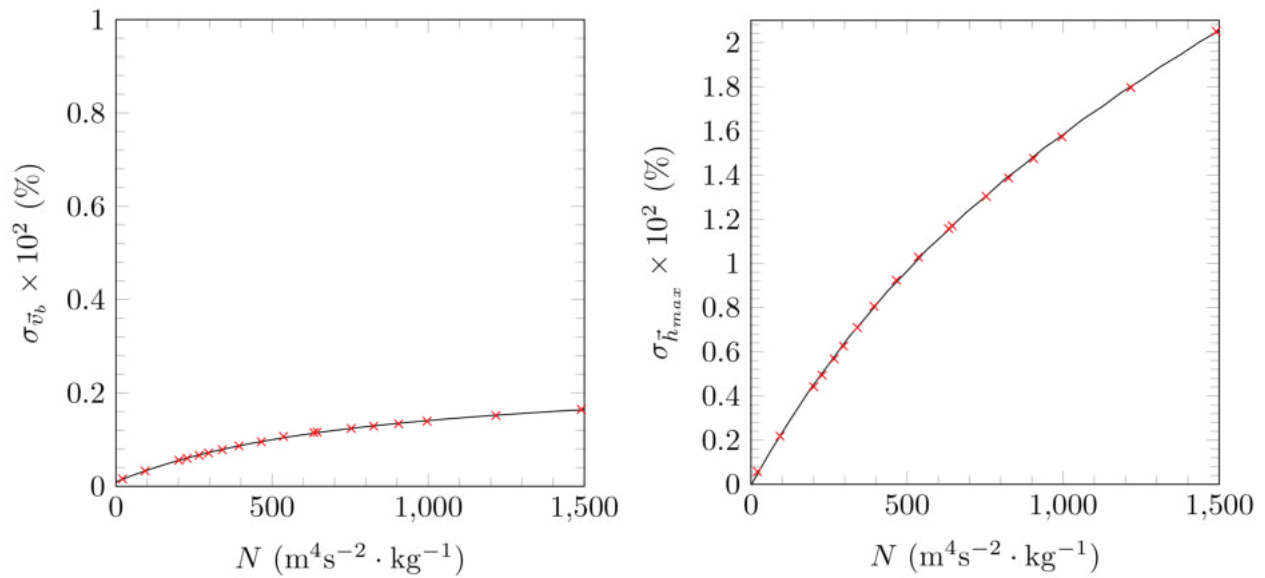


Figure 14: Graphs showing scatter plots alongside their lines of best fit for burnout velocity $\sigma \vec{v}_b$ and $\sigma \vec{h}_{max}$ against N .

The equations for the lines of best fit for best fit are the following:

$$\sigma \vec{v}_b(N) = 1.2704 \times 10^{-1} - 1.1749 \times 10^{-1} \times (9.9791 \times 10^{-1})^N + 2.8306 \times 10^{-5}N \quad (27)$$

$$\sigma \vec{h}_b(N) = 1.0329 - 1.0369 \times (9.9826 \times 10^{-1})^N - 7.3118 \times 10^{-4}N \quad (28)$$

As it can be observed, the burnout velocity suffers deviations of up to 16.5% from our trials, whereas the maximum altitude suffers deviations as great as 205.0%. This is because the burnout velocity is achieved after the rocket has been impulsed due to the thrust provided by the motor, and the relatively large thrust to weight ratios (Ψ_0) make the impact of drag relatively small during the short period of time it is being powered. However, the burnout altitude suffers great losses due the lack of thrust, this is because the energy the rocket has to achieve its maximum altitude is determined by the kinetic velocity the rocket has at burnout given by:

$$E_{K_b} = \frac{1}{2}M_f\vec{v}_b^2 \quad (29)$$

In Figure 13 we have seen how large the magnitude of the drag force acting on the rocket can get at high velocities. Both gravity and the drag force slow the rocket down without any sort of resistance from the rocket since thrust is no longer present until its $E_K = 0$, and thus, reductions in the maximum altitude are much higher. In addition, much of the rocket's kinetic energy is also transferred to thermal energy, which might heat the rocket to significant temperatures, and could result in structural damage, depending on the heat capacity of the material the rocket is built from.

These significantly large reduction factors as well as their deviation would add a layer of uncertainty to the flight of a rocket in experimental conditions which might have not been taken into account in the simulator, being one of the greatest limitations of this investigation.

The fact that this investigation was carried out through a simulator rather than through experimentation, means that some other additional factors need to be considered in order to achieve a rocket with the capabilities of achieving high altitudes and velocities in order to achieve a stable

flight that results in the maximum possible performance. The following subsections will explore some of these aspects.

4.2.1 Transonic and Supersonic Flight

The technical documentation for the simulator states the following:

“Since the analytical prediction of aerodynamic properties in the transonic³ region is quite difficult, this region will be accounted for by using some suitable interpolation function that corresponds reasonably to actual measurements.” (Niskanen)

This could imply that some of our rockets were so light in mass that they were able to achieve speeds within the transonic and supersonic regions, which could add some uncertainty to the model, however, we will consider this effect as negligible due to the given justification.

³Mach 0.8 - 1.2

4.3 Flight Stability

Since no wind was simulated for the flight of the rockets, this meant that there would be no turbulence acting upon the rockets, this is once again a very ideal situation, since on a practical situation, some wind would most likely be present when launching a rocket. The effect that wind has on the rocket is very significant since, if the rocket does not have a meticulous stability, even the slightest gust of wind could deviate its trajectory and completely send it off course.

Stability is the tendency the rocket has to restore itself to its original condition after being disturbed, and it is therefore very important to make a stable rocket in order for the experimental results to match the theoretical calculations.

4.3.1 Aerodynamic Stability

Aerodynamically, the stability would remain constant for all variations of the rocket, since it is only dependent on the exterior surfaces, and since these would not vary, it would not affect each variation.

The rocket was designed to be as streamlined as possible, where radial symmetry of the design of the rocket and the lack of unnecessary protruding surfaces reduced the amount of unnecessary drag to a great extent.

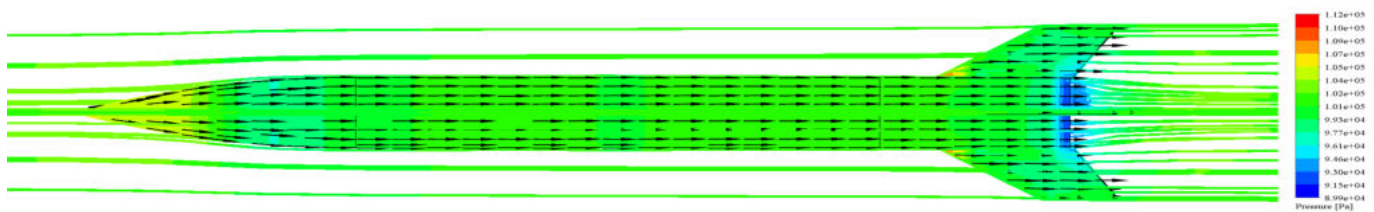


Figure 15: SOLIDWORKS Flow Simulation (Dassault Systèmes) results of the rocket coasting at 250 ms^{-1} , the color mappings represent the pressure acting upon the body in Pascals (Pa), as indicated by the colorbar on the right.

The simulation results further back this claim, as we can see, the airflow is streamlined as it travels down the body of the rocket, the pressure is also well distributed, with the only higher pressure zones being naturally the tip of the nosecone and the tips of the fins, since these are the protrusions that first come in contact with the air and hence create disturbances that result in

these high pressures, however, since these pressures were evenly distributed, and hence, they were low enough not to cause structural damage on most materials, however, this is heavily dependent on the material used, where a higher strength material will have higher pressure tolerance and hence better cope with the resultant force.

4.3.2 Static Stability

Unlike aerodynamic stability, static stability does not depend on the aerodynamic, but rather on the centres of pressure and gravity of the rocket. The center of gravity is the point in the body where all mass is concentrated, whereas the center of pressure is the point where all air pressure forces concentrate about.

Both the center of mass and the center of pressure vary throughout the rockets flight. The center of mass shifts position as rocket is burnt, this shift can be quite significant since much of the rocket's weight in some cases could be the fuel its carrying. The center of pressure on the other hand, changes with the angle of attack of the rocket, since the local pressure at every point on the aerofoil also changes (SKYbrary), if the flight of the rocket remains vertical for the entirety of the flight, theoretically, the center of pressure should not shift position, since there is no variation in its angle of attack.

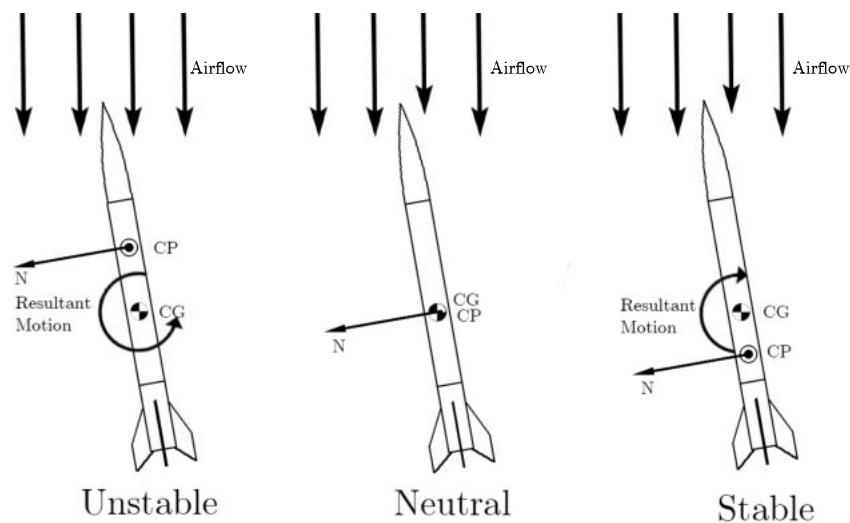


Figure 16: Graphical representation of how the distance between the center of gravity and the center of pressure affects the static stability of the rocket.

If the center of pressure is above the center of mass, when the force acts upon the center of mass, this will completely throw it off balance and the rocket will not be able to recover back to its vertical position after being deviated. On the other hand, if the center of mass is above the center of pressure, the rocket will be able to stabilize itself back to its vertical position.

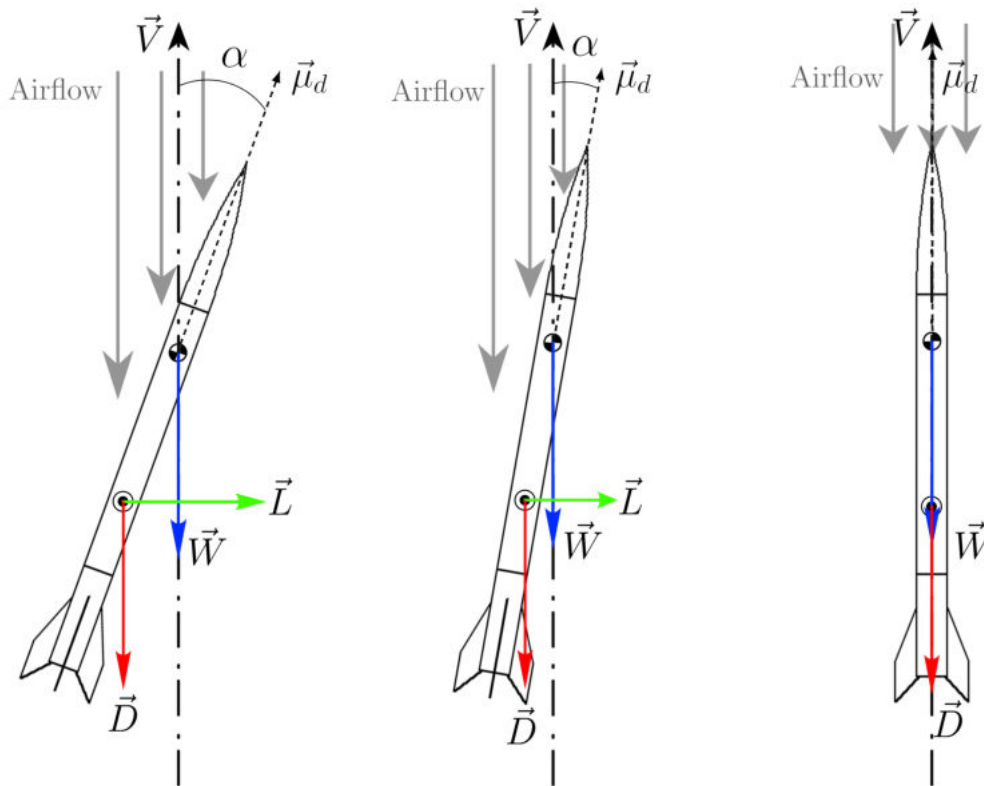


Figure 17: Diagram showing the passive stabilization of an unpowered rocket during the coasting phase flying at velocity \vec{V} with its nosecone pointing towards the direction vector $\vec{\mu}_d$.

As we can see from the previous diagram, a stabilizing rocket produces a normal lift force \vec{L} perpendicular to the drag force \vec{D} of the rocket, which corrects the rocket's trajectory due to the restoring moment it generates when wind impacts the rocket laterally. The angle α , shows the rocket's angle of attack, which is the angle at which it is pitched at, being the angle formed between the vertical across its center of mass and the nosecone direction vector $\vec{\mu}_d$. The magnitude of the lift force is directly proportional to the magnitude of the angle of attack (NASA):

$$\vec{L} = \frac{C_L \rho \vec{V}^2 A}{2} \quad (30)$$

Where C_L is the lift coefficient, and A is the total surface area of the rocket coming into contact with the airflow. The larger the angle of attack is, the larger the total surface area in contact with the air will be, and hence, a greater lift force will be produced.

A statically stable rocket is of great interest for when the rocket enters the coasting phase, where it no longer has a force (thrust) that allows it to remain flying at an ideally constant angle of attack of 0° if the conditions allow it.

However, static stability only considers instantaneous time frames, and since the rocket has a changing momentum, this means that adjusting to a stable position would take time, and this is not taken into account, being the main limitation behind only using the static margin to determine stability. Dynamic stability could also be employed, however, its complexity leaves it out of the scope of the investigation.

A way to measure the static stability of our rockets is by calculating the static margin of each at the burnout instance. The static margin is the distance between the CP and the CG (Barrowman), given by the following equation:

$$\kappa_{SM} = X_{CP} - X_{CG} \quad (31)$$

Where X_{CP} is the distance from the tip of the nosecone to the center of pressure and X_{CG} to the center of gravity, and it is a dimensionless quantity.

Rocket	ρ_s (gcm^{-3})	κ_{SM}
A	0.76	1.373
B	0.85	1.625
C	0.95	1.865
D	1.00	1.955
E	1.05	2.020
F	1.10	2.067
G	1.19	2.116
H	1.20	2.121
I	1.30	2.130
J	1.39	2.114
K	1.50	2.114
L	1.60	2.092
M	1.70	2.068
N	1.78	2.048
O	1.85	2.031
P	1.90	2.019
Q	2.00	1.997
R	2.70	1.904
S	4.50	1.520

Table 9: Table showing the calculated static margin using Equation 31 and structural material density of each rocket.

All rockets flown in this investigation were stable since $\kappa_{SM} > 0$. The greater the static margin is, the more stable the rocket will be, however, a rocket that is too stable might favor a phenomena called weather cocking which will be discussed in section 4.4.2, since corrections in the trajectory could have too much restoring moment. The ideal static margin of a rocket would be approximately equal to its diameter (Barrowman).

4.4 Flight Trajectory Deviations

Our pursuit during this investigation was to investigate the aerodynamic effects acting upon a rocket flying through a vertical trajectory, however, as we have explored in section 4.3.2, the presence of air itself could deviate the trajectory of rocket if its center of pressure and gravity are not property balanced.

The fact that the rocket was flying in a vertical trajectory for our theoretical value calculations and simulations implied that there was a single component in which force was acting upon the rocket, that being the y component, from our non-inertial frame of reference.

4.4.1 Two-Dimensional Flight

Even though this investigation does not focus on two- dimensional flight, it may seem relevant to show how this system of equation would function.

At any given instance of time:

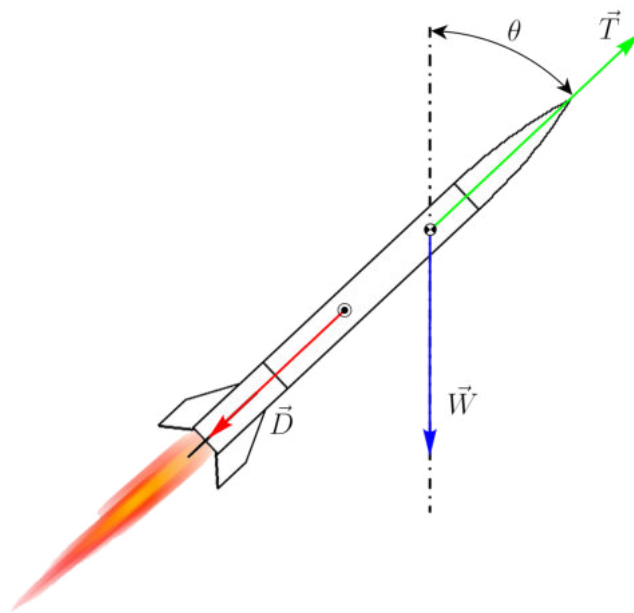


Figure 18: Free body diagram of a rocket flying at an angle θ at an instantaneous moment of time.

The acceleration as a function of time can be obtained from the equation of motion $M \frac{d\vec{V}}{dt} = \vec{T} + \vec{W} + \vec{D}$, which yields (Keepports):

$$\vec{a}(t) = \frac{\vec{T}(t) + \vec{W}(t) + \vec{D}(t)}{M(t)} \quad (32)$$

The horizontal and vertical components of \vec{a} are given by:

$$a_x(t) = \vec{a}(t) \cdot \cos[\theta(t)] \quad (33)$$

and

$$a_y(t) = \vec{a}(t) \cdot \sin[\theta(t)] \quad (34)$$

To then find the horizontal and vertical velocity components after a time interval denoted as Δt after time t :

$$v_x(t + \Delta t) = v_x(t) + a_x(t)\Delta t \quad (35)$$

and

$$v_y(t + \Delta t) = v_y(t) + a_y(t)\Delta t \quad (36)$$

Knowing the velocity components, we may now determine the horizontal and vertical distances travelled by employing the following equations:

$$\vec{x}(t + \Delta t) = \vec{x}(t) + v_x(t)\Delta t \quad (37)$$

and

$$\vec{y}(t + \Delta t) = \vec{y}(t) + v_y(t)\Delta t \quad (38)$$

4.4.2 Implication of the Presence of Wind

Wind has still not been taken into account in these equations. If there was a lateral wind that acted upon the rocket during its ascent or coasting phase, this could tremendously impact its trajectory, as the rocket could start flying at an angle, and an x component would be added to the forces acting upon the rocket. This phenomena is known as *weather cocking*.

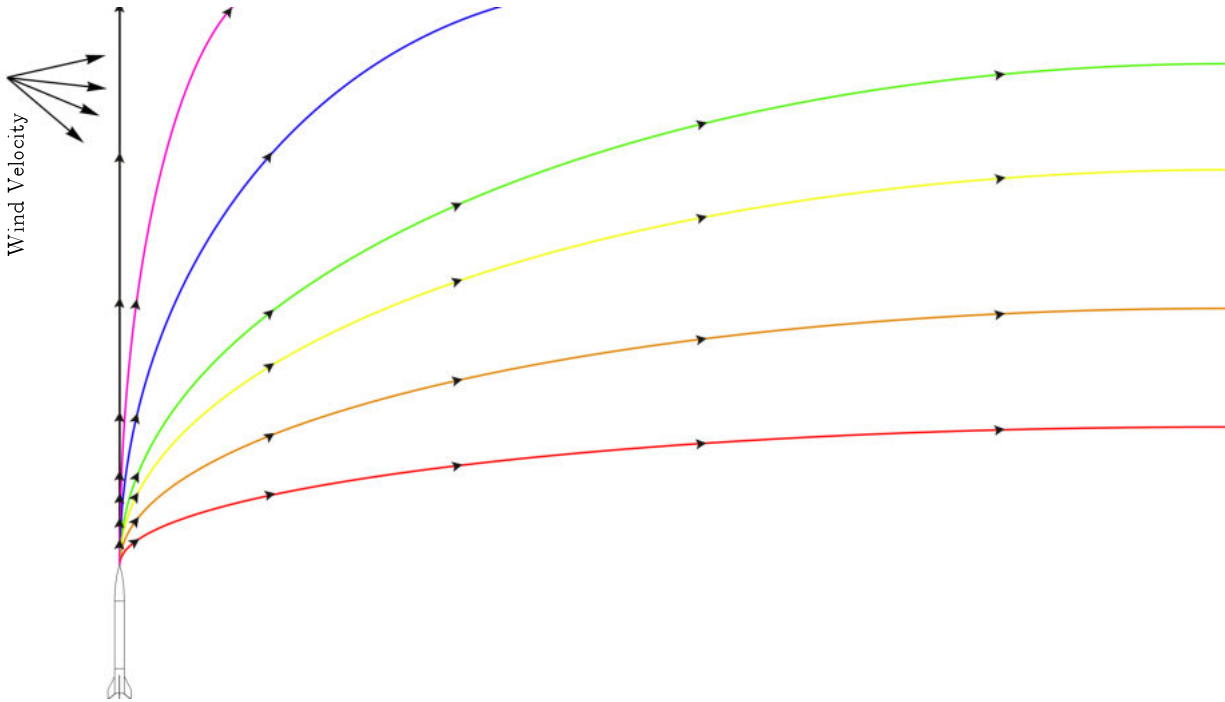


Figure 19: Graphic showing the different trajectories a rocket could take depending upon the velocity of the wind. (Not to scale)

A numerical analysis of the effects of wind would unfortunately go far beyond the scope of investigation, due to the extreme complexity of wind, since it arbitrarily varies in direction, magnitude, viscosity and many other aspects, thus, this investigation is only valid for rockets flying with a null windspeed.

5 Conclusion

By changing the density of the rocket's structural material, we obtained rockets with final masses ranging from 50.54kg to 196.25kg. The shape of these rockets remained constant, with a drag coefficient of 0.36, and diameter of 0.225m, providing them with a constant thrust of 8034.5N for 5.12s which resulted in drag influence numbers ranging from 1490.4 to 20.9. Analyzing the created model showed how the reduction factors for the rockets ranged between 0.86 to 0.98 for their burnout velocities and 0.33 to 0.95 for their maximum heights, with their respective deviations ranging from 16.5% to 1.6% and 200.5% to 5.7%

Lightweight rockets achieved the highest velocities and altitudes whilst having the largest reduction factors and deviations from their theoretical values due to the increased drag force acting upon them since $\vec{D} \propto \vec{V}^2$, whereas heavier ones had lower velocities and altitudes, but lower reduction factors and deviations. Determining the 'optimal' drag influence number is heavily dependent on the application of the rocket, where a rocket looking to achieve maximum velocities and heights might want a low mass to increase its N at the cost of having a less reliable theoretical value adding a greater uncertainty, whereas rockets aiming to minimize the effects of drag might want a lower N at the cost of reduced velocities and altitudes.

Further investigations could be carried out by utilizing parameter N , where the mass of the rocket could be kept constant and other aspects of the rocket could be varied, such as its drag coefficient. The results from these could then be compared to verify the validity of this model. A two-dimensional model could also be created based on the established theoretical framework, where the angle at which the rocket is launched could be varied.

6 Bibliography

References

- Ambrosius, B.A.C, R.J Hamann, and K.F Wakker. *Introduction to Aerospace Engineering*. TU Delft OpenCourseWare, Feb. 2016. Visited on 03/20/2020. https://ocw.tudelft.nl/wp-content/uploads/AE1102_Space_Slides-9-10.pdf.
- Barrowman, Jim. “Stability of a Model Rocket in Flight”. *Technical Information Report*, no. 30 (1988): 10–11. Visited on 09/01/2020. <http://www.rockets4schools.org/images/Rocket.Stability.Flight.pdf>.
- Dassault Systèmes. *Solidwoks SP 3.0*. Solidworks, 2018. Visited on 06/29/2020. <https://www.solidworks.com/>.
- David, John. *Introduction to flight*. 3rd ed. 513–514. Mcgraw-Hill, 1989. ISBN: 0-07-001641-0.
- Flight of a Rocket*, Mar. 2021. Visited on 03/10/2021. https://osf.io/wzm6h/?view_only=451240c44a904ab8bee03918b2603d66.
- Keeports, David. “Numerical calculation of model rocket trajectories”. *The Physics Teacher* 28 (May 1990): 274–280. Visited on 11/05/2020. <https://doi.org/10.1119/1.2343024>.
- Nakka, Richard. *Simplified method for estimating the flight performance of a hobby rocket* (Mar. 2007). Visited on 03/23/2020. <https://www.nakka-rocketry.net/articles/altcalc.pdf>.
- NASA. *The Lift Equation*. Nasa.gov, 2015. Visited on 09/01/2020. <https://www.grc.nasa.gov/www/k-12/airplane/lifteq.html>.
- Niskanen, Sampo. *OpenRocket Simulator*, May 2020. Visited on 03/16/2020. <http://openrocket.info/>.
- . “OpenRocket technical documentation”. *Development of an Open Source model rocket simulation software* (May 2013): 28. Visited on 04/09/2020. http://www.printedrockets.com/uploads/6/9/7/9/6979786/openrocket_techdoc.pdf.

SKYbrary. *Centre of Pressure*, July 2017. Visited on 08/29/2020. https://www.skybrary.aero/index.php/Centre_of_Pressure.

Young, Trevor. *Performance of the Jet Transport Airplane: Analysis Methods, Flight Operations, and Regulations*. 1st ed. 583–590. Wiley, Oct. 2017. ISBN: 978-1-118-38486-2.

7 Appendix

7.1 Derivation of Equation 3

(Ambrosius, Hamann, and Wakker)

We first consider the rocket to be flying with no external force acting upon it (nor gravity nor drag), following Newton's Second Law, the total impulse remains constant:

$$\frac{d\vec{I}}{dt} = 0$$

Therefore,

$$\vec{I}_t = M\vec{V}$$

$$\vec{I}_{t+\Delta t} = (M + \Delta M)(\vec{V} + \Delta\vec{V}) - (\vec{V} - \vec{w})\Delta M$$

so;

$$\begin{aligned} \frac{\Delta\vec{I}}{\Delta t} &= \frac{\vec{I}_{t+\Delta t} - \vec{I}_t}{\Delta t} \\ &= M\frac{\Delta\vec{V}}{\Delta t} + \vec{w}\frac{\Delta M}{\Delta t} + \frac{\Delta M\Delta\vec{V}}{\Delta t} \end{aligned}$$

$$\lim_{\Delta t \rightarrow 0} \left(M\frac{\Delta\vec{V}}{\Delta t} + \vec{w}\frac{\Delta M}{\Delta t} + \frac{\Delta M\Delta\vec{V}}{\Delta t} \right) = \frac{d\vec{I}}{dt} = M\frac{d\vec{V}}{dt} + \vec{w}\frac{dM}{dt}$$

or

$$M\frac{d\vec{V}}{dt} = -\vec{w}\frac{dM}{dt}$$

and

$$d\vec{V} = -\vec{w}\frac{dM}{M} \quad \text{or} \quad M\frac{d\vec{V}}{dt} = -\vec{w}\dot{m}$$

The external forces of gravity and drag are now introduced into the equation:

$$d\vec{V} = -\vec{w}\frac{dM}{M} - \vec{W} - \vec{D}$$

$$= -\vec{w} \frac{dM}{M} - M\vec{g} - \vec{D}$$

Which becomes:

$$d\vec{V} = -\vec{w} \frac{dM}{M} - \vec{g} dt - \frac{\vec{D}}{M} dt$$

7.2 Data and File Repository

Since the data exported from each simulator flown was excessive to attach to this document. It has been uploaded to a file repository through the Center for Open Science organization (*Flight of a Rocket*), alongside other relevant files utilized during this investigation, such as the CAD models for the rockets.

- The file containing all exported flight data is titled “FlightData.xlsx”
- A file containing the CAD model has also been uploaded to the same repository, titled “Rocket Assembly.SLDPRT”

The URL to the complete repository is the following:

https://osf.io/wzm6h/?view_only=451240c44a904ab8bee03918b2603d66